ISSN:3007-9640 DOI: https://doi.org/10.70114/acmsr.2025.3.1.P284

Research on CPU waste heat utilization system of CAES coupled oxyfuel coal-fired unit

Zhiyu Zhang [1, a] , Haihui Song [1, b]*

[1] School of Energy and Environment,Inner Mongolia University of Science and Technology，Baotou 014010, China

[a] zzy0021@126.com [b]1669034368@qq.com

Abstract. In order to reduce carbon emission and increase flexibility of thermal power units, a new power system of compressed air energy storage coupled with oxyfuel coal-fired units using CPU waste heat(CFPP+CAES+CPU) was proposed. Using Ebsilon Professial and Aspen Plus software to build a model, the thermodynamic characteristics and economic analysis of the system were carried out. The results show that: In fixed coal consumption mode, the exergic power of CFPP+CAES+CPU unit increased by 0.745% at the lowest and 1.216% at the highest. Exergic damage of exergic power of CFPP+CAES+CPU unit decreased compared with control unit, while exergic efficiency of heat exchanger in CPU increased. The maximum economic mode of CFPP+CAES+CPU unit is that when CO2 and carbon emission rights are sold, the minimum LCOE is 0.374¥/kWh when carbon tax is not considered.

Keywords: compressed air energy storage; oxyfuel combustion; waste heat utilization

1. Introduction

Coal-fired power plants release about 33% of the world's CO2 emissions[1]. In terms of reducing carbon dioxide emissions of coal-fired power plants, oxyfuel combustion technology can be applied to existing coal-fired power plants and is one of the most promising technologies for CO2 capture in the power generation industry[2].

Thermal power units realize load regulation by frequently changing unit working conditions, which not only has poor flexibility, but also easily affects the reliability and efficiency of unit operation[3]. The coupling of thermal power unit and energy storage system can realize the "decoupling of furnace and machine", which is an important way to improve the flexibility of thermal power operation[4]. For example, literature [5] analyzed a 660MW thermal power unit with a coupled molten salt energy storage system, indicating that the addition of molten salt energy storage system can effectively improve the reaction rate of thermal power units to grid load. Literature [6] established a hierarchical optimal scheduling model for combined pump-storage and thermal power peak regulation, and concluded that the economy of thermal power peak regulation can be increased when coupled with pumped storage. Literature [7] analyzes the possible coupling mode between a 660MW thermal power unit and the compressed air energy storage (CAES) system. It is concluded through thermodynamic analysis that the cycling efficiency of the CAES system increases to 78.85% when coupled with CAES. The maximum output of thermal power was also increased. However, when coupled with CAES, the above schemes need to extract part of the low-temperature and high-pressure air from the thermal power unit to preheat the low-temperature and high-pressure air in the CAES energy release stage, which is not conducive to the stable operation of the thermal power unit and also reduces the turbine output capacity of the unit at this time, and the peak load capacity of the unit has potential to be improved. In exploiting this potential, Li Bin et al. [8] proposed to use solar energy and molten salt energy storage to preheat the air when releasing energy in CAES, which improved the stability of thermal power units, but it correspondingly increased the cost and did not conduct an overall economic calculation. Considering that the gas compression and purification unit (CPU) in the oxyfuel coal-fired unit will also produce a large amount of waste heat, this part of waste heat should be replaced by the steam turbine preheating and pumping. Using low grade heat source can also increase the output capacity of steam turbine. Therefore, based on the principle of temperature gradient utilization, this paper

ISSN:3007-9640 DOI: https://doi.org/10.70114/acmsr.2025.3.1.P284

uses Ebsilon and Aspen Plus to establish the CPU waste heat utilization model of CAES coupled oxyfuel coal-fired unit, and studies its thermal characteristics and economic analysis.

2. System Description

The process flow of the CAES coupled oxygen-enrichment unit scheme (baseline scenario) is shown in Figure 1. According to Table 1, the coupled unit is divided into three operation stages within a day. Among them, the off-peak period operation lasts for 8 hours, with control valves RV3 and RV4 closed, CAES in the energy storage stage, and part of the turbine output power of the oxygen-enrichment unit drives the compressor of CAES to compress and store the air into the high-pressure storage tank. During this period, control valves RV1 and RV2 are opened, and part of the condensate water enters the heat exchanger to recover the residual heat of the compressor and then enters the boiler; the peak period operation lasts for 4.382 hours, with control valves RV1 and RV2 closed, CAES in the energy release stage, and the low-temperature high-pressure air released from the high-pressure storage tank enters the turbine to do work. During this period, control valves RV3 and RV4 are opened, and part of the turbine exhaust gas enters the heat exchanger to preheat the low-temperature high-pressure air; during the off-peak period, CAES stops working.

The CPU waste heat utilization scheme of the CAES coupled oxyfuel coal-fired unit (CFPP+CAES+CPU) is different from the control scheme in the CAES energy release stage. By using the flue gas from the CPU compressor to replace the turbine exhaust gas preheating the inlet of the turbine in the baseline scenario, the output power of the turbine is improved and the energy utilization capacity of the system is enhanced; at the same time, during the CAES energy storage stage and when it is not working, by connecting the heat exchanger H9 in parallel with L1, the reduction of the exhaust gas entering the return heat system increases the output power of the turbine. It is worth noting that under the heat exchange conditions of the new heat exchanger, there is a range of waste heat recovery of the CPU compressor by controlling the condensing water entering the new heat exchanger.

Table 8.Time-of-Use Electricity Pricing[9]

Parameter	Time Period	Price/(¥·(kW·h)$^{-1}$)
Peak Period Price	10:00-15:00/18:00-21:00	1.264
Flat Period Price	7:00-10:00/15:00-18:00/21:00-23:00	0.7453
Off-Peak Period Price	23:00-07:00(next day)	0.2779

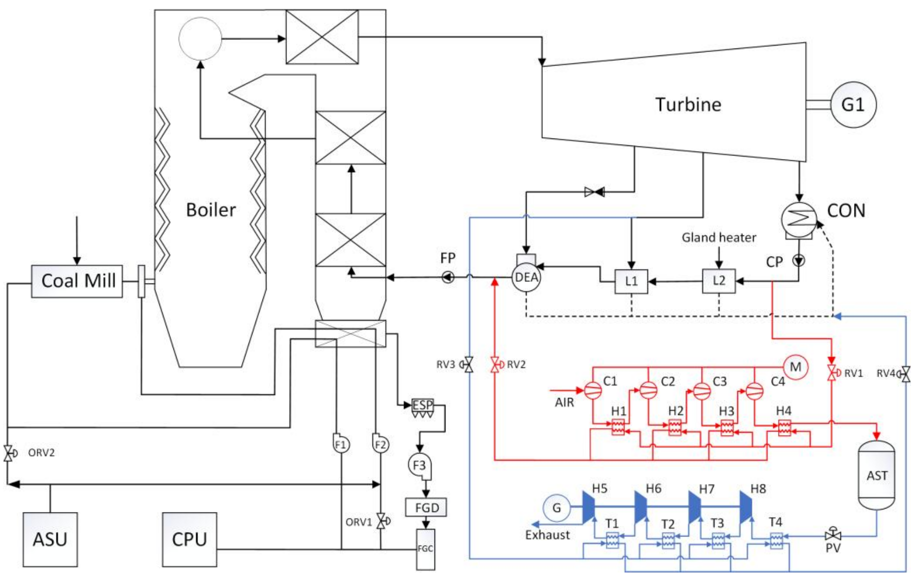

Fig.1 Flow chart of CAES coupled oxyfuel unit

ISSN:3007-9640 DOI: https://doi.org/10.70114/acmsr.2025.3.1.P284

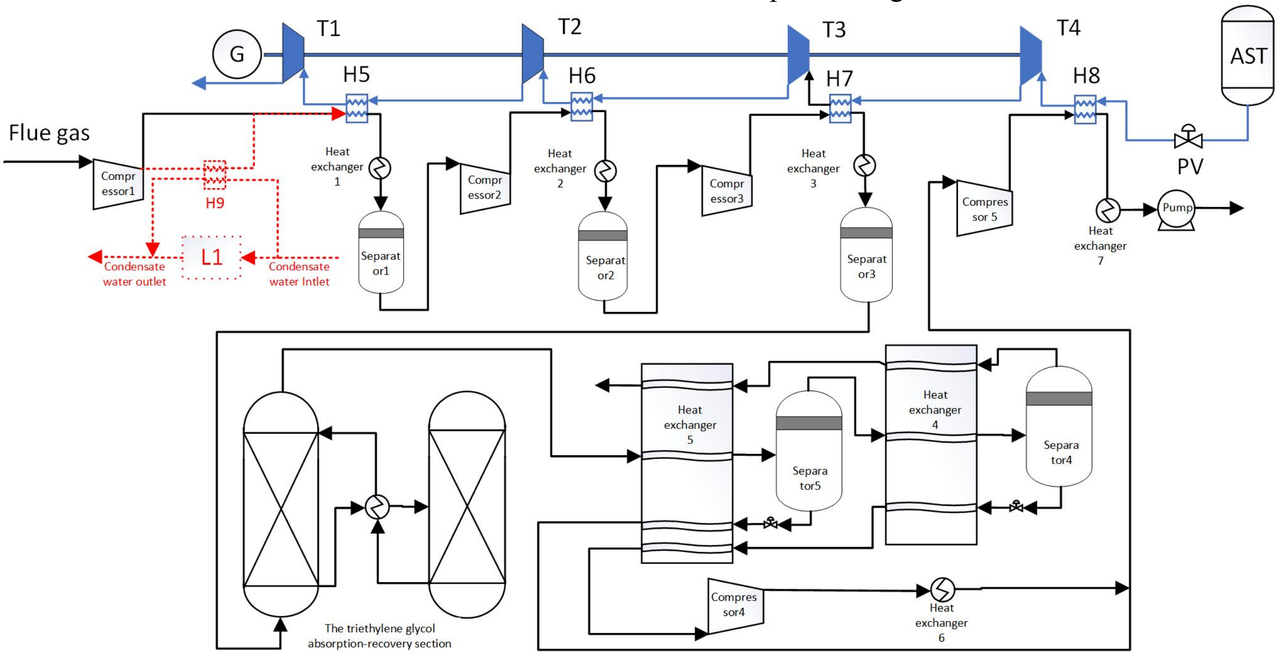

Fig.2 Schematic diagram of the energy release stage of CFPP + CAES + CPU

3. Result and Discussion

3.1 Model Assumptions

To simplify the subsequent analysis process, the following assumptions are made for the CPU waste heat utilization system:

(1) The coupled system operates in a fixed coal consumption mode.

(2) The composition of air is 75.53% N_2, 23.14% O_2, 1.29% Ar, and 0.4% CO_2 (by mass fraction).

(3) The pipeline pressure drop and heat loss in the CAES are neglected.

(4) The unit operates under steady-state conditions.

(5) The throttling process of air is considered an isenthalpic process.

(6) By adjusting the airflow rate, the CAES output is maintained at 10% of the oxyfuel unit load [19].

3.2 Model Establishment

Based on the above assumptions, the energy balance equation of the boiler is[11]:

$$\mathrm{m_{coal}LHV_{coal}\eta_b = m_{sh}(h_{sh} - h_{fw})} \quad (1)$$

In the formula,$m_{coal}$is the coal consumption;$LHV_{coal}$is the lower heating value of the fuel;$\eta_b$is the boiler thermal efficiency;h_{sh} and $h_{fw}$are the enthalpies of superheated steam and boiler feedwater, respectively.

The calculation formula for the output power of the stage group through-flow section is as follows[11]:

$$P_{oxyfuel} = \sum_{m=1}^{M} \eta_s^m \left(D_{s,in}^m \cdot h_{s,in}^m - D_{s,out}^m \cdot h_{s,out}^m - D_e^m \cdot h_e^m\right) \quad (2)$$

In the formula,$P_{oxyfuel}$represents the oxyfuelunit's turbine output power;η_s^mdenotes the efficiency of the m-th stage turbine unit;$D_{s,in}^m$ and $D_{s,out}^m$are respectively the inlet and outlet mass flow rates of the m-th stage unit;$h_{s,in}^m$ and $h_{s,out}^m$correspond to the inlet and outlet steam enthalpy values of the m-th stage;D_e^mindicates the extraction steam mass flow rate at the m-th stage;h_e^m represents the extraction steam enthalpy value at the m-th stage.

The calculation formula for compressor power consumption is as follows [11]:

$$P_{c,i} = m_{c,i}\left(h_{cout,i} - h_{cin,i}\right) \quad (3)$$

ISSN:3007-9640 DOI: https://doi.org/10.70114/acmsr.2025.3.1.P284
In the formula, i denotes the i-th stage compressor; $m_{c,i}$ represents the air flow rate at the inlet of the i-th stage compressor;$h_{cout,i}$ and $h_{cin,i}$ represent the enthalpy values at the outlet and inlet of the compressor,respectively.

The turbine output power calculation formula is expressed as [11]:

$$P_{t,i} = m_{t,i}(h_{tin,i} - h_{tout,i}) \tag{4}$$

In the formulation, j denotes the i-th stage compressor; $m_{t,i}$ represents the air flow rate at the inlet of the i-th stage compressor;$h_{tin,i}$ and $h_{tout,i}$ represent the enthalpy values at the outlet and inlet of the compressor,respectively.

The heat exchanger calculation formula is expressed as [11]:

$$Q_{HX} = m_{hot}|h_{hot,out} - h_{hot,in}| = m_{cool}|h_{cool,out} - h_{cool,in}| \tag{5}$$

In the formulation,Q_{HX}denotes the heat exchanger capacity;m_{hot} and m_{cool}represent the hot-side and cold-side working fluid mass flow rates, respectively. $h_{cool,in}$ and $h_{cool,out}$ denote the cold-side working fluid enthalpy values at the inlet and outlet of the heat exchanger, respectively;$h_{hot,in}$ and $h_{hot,out}$ represent the hot-side working fluid enthalpy values at the inlet and outlet of the heat exchanger.

3.3 Performance indicators

3.3.1 Heat rate

To investigate and evaluate the thermal economic performance of the coupled system, this study adopts heat rate as the evaluation metric. The governing equation is formulated as follows[8]:

$$q = \frac{D_{gs} \times H_{gs}}{P_{grid}} \tag{6}$$

In the formula:$\mathrm{q}$is the heat rate,kJ/kWh;$\mathrm{D_{gs}}$denote the feedwater mass flow rate, reheat steam mass flow rate, and heating extraction steam mass flow rate,kg/s;$\mathrm{H_{gs}}$represent the feedwater enthalpy rise, reheat steam enthalpy rise, and heating extraction enthalpy rise,kJ/kg.

3.3.2 Exergy Efficiency and Exergy Destruction

Exergy efficiency quantifies the utilization ratio of available energy in components or systems, assessing the remaining potential for improving energy conversion effectiveness. The exergy efficiency equation for the i-th component/system is formulated as:

$$\eta = \frac{\mathrm{E_i^P}}{\mathrm{E_i^F}} \tag{7}$$

Exergy destruction quantifies the thermodynamic penalty during energy conversion processes. The governing equation is formulated as:

$$\mathrm{E_i^D} = \mathrm{E_i^F} - \mathrm{E_i^P} \tag{8}$$

In the equation:$\mathrm{E_i^F}$denotes the input exergy of the i-th component during the exergy transformation process; $\mathrm{E_i^P}$ represents the exergy product; $\mathrm{E_i^D}$ indicates the inevitable exergy destruction due to thermodynamic irreversibilities.

3.3.3 Levelized Cost of Energy

Levelized Cost of Energy (LCOE) is an indicator used to measure the average cost per kilowatt-hour of electricity generated by a power generation project throughout its entire life cycle, taking into account all costs (including construction costs, operating costs, fuel costs, etc.) and the electricity produced. The formula is as follows [2]:

$$\mathrm{LCOE} = \left(\mathrm{I_{cc}} + \sum_{n=1}^{N} \frac{\mathrm{Cost_{ann,n}}}{(1+\mathrm{r_{dis}})^n}\right) \Big/ \left(\sum_{n=1}^{N} \frac{\mathrm{P_{gen,n}}}{(1+\mathrm{r_{dis}})^n}\right) \tag{9}$$

In the equation:$\mathrm{I_{cc}}$ represents the capital cost of the coupled system;$\mathrm{Cost_{ann,n}}$ represents the cost in the n-th year;$\mathrm{P_{gen,n}}$ represents the electricity generation in the n-th year;$\mathrm{r_{dis}}$ represents the discount rate.

ISSN:3007-9640 DOI: https://doi.org/10.70114/acmsr.2025.3.1.P284

4. Result and Discussion

4.1 Model Validation

The oxyfuel boiler in this study was validated against experimental data from the 35 MWth oxy-fuel boiler in Reference [13], with steam turbine model N7.5-3.43. The CPU parameters were consistent with Reference [14], and the ASU employed a triple-column process with parameters adopted from Reference [15]. The coal ultimate and proximate analyses matched those in Reference [13]. A comparison between model simulations and reference data is presented in Table 1, where the main steam pressure is specified as the setpoint value.

Table 1 Model validation table

Parameter		Reference Value	Simulated Value
oxyfuel boiler[13]	High-temperature superheater outlet gas temperature/°C	660	658.51
	Flue gas temperature/°C	130	129.81
	Main steam temperature/°C	420	420.37
	Main steam pressure/MPa	3.22	3.22
CAES[8]	Compressor power consumption/MW	9.62	9.671
	Expander output power/MW	10.03	10.03
	RTE	52.572	52.572
CPU[14]	Recovery rate/%	94.7	94.672
	Total energy consumption/MW	63.59	63.558
ASU[15]	Total energy consumption/ kW	35106	35089
	Specific ASU power/($kWh\cdot t^{-1}O_2$)	304.6	304.5

The simulated values exhibit minimal deviations from reference data. This demonstrates that the model satisfies the accuracy requirements for thermodynamic analysis and can be reliably applied to subsequent studies.

4.2 Thermodynamic Characteristics

Table 2 presents the thermodynamic performance comparison between the two schemes. The maximum waste heat recovery capacity of the CPU compressor is achieved in each case.

During the peak electricity consumption period, the output power of the CAES in both schemes is 750 kW. In terms of the output power of the steam turbine, in the CFPP+CAES+CPU scheme, the flue gas is utilized to replace the steam extraction from the steam turbine for preheating the low-temperature and high-pressure air released by AST, resulting in an increase in the steam flow through the steam turbine's flow passage. Consequently, the output power of the steam turbine in the CFPP+CAES+CPU scheme is 90.096 kW higher than that in the control scheme, with an increase of 1.216%. Regarding the heat consumption rate, the CFPP+CAES+CPU scheme reduces it by 114.494 kJ/kWh, a decrease of 1.036%. This is because the heat consumption rate decreases as the output power of the unit increases. During this process, the CFPP+CAES+CPU scheme recovers 755.55 kW of CPU flue gas waste heat.

During the off-peak electricity consumption period, the input power of the CAES in both schemes is also 750 kW. In terms of the output power of the steam turbine, in the CFPP+CAES+CPU scheme, by paralleling the additional heat exchanger with the low-temperature heat exchanger L1, the steam flow through the steam turbine's flow passage is further increased. As a result, the output power of the steam turbine in the CFPP+CAES+CPU scheme is 56.584 kW higher than that in the control scheme, with an increase of 0.745%. Regarding the heat consumption rate, the CFPP+CAES+CPU scheme reduces it by 99.512 kJ/kWh, a decrease of 0.756%. During this process, the CFPP+CAES+CPU scheme recovers 399.985 kW of CPU flue gas waste heat.

ISSN:3007-9640 DOI: https://doi.org/10.70114/acmsr.2025.3.1.P284

During the flat electricity consumption period, in the CFPP+CAES+CPU scheme, only the additional heat exchanger is paralleled with the low-temperature heat exchanger L1, but the recovered CPU waste heat is 400.746 kW, which is higher than that during the off-peak period. The reason lies in that the amount of condensate water entering the additional heat exchanger is slightly higher than that during the off-peak period.

Table 2 Compares the thermal performance of the two schemes

Parameter	Peak Load Period		Off-Peak Load Period		Off-Peak Period Price	
	baseline scenario	CFPP+CAES+CPU	baseline scenario	CFPP+CAES+CPU	baseline scenario	CFPP+CAES+CPU
Steam Turbine Output/kW	7409.904	7500	7595.429	7652.013	7500	7555.241
CAES Power/kW	750	750	750	750	0	0
Heat Rate/kJ·(kW·h)$^{-1}$	11050.002	10935.508	13170.922	13071.41	12029.059	11941.108
Total System Output/kW	8164.518	8250	6849.864	6902.013	7500	7555.241
CPU Waste Heat Recovery/kW	0	755.55	0	399.985	0	400.746

4.3 Exergy Analysis

Figure 3 shows the exergy efficiency comparison of CAES components of the two schemes. It can be seen from the figure that the exergy efficiencies of the compressor, turbine, and throttle valve of the two schemes are the same, and only H5-H8 are different. For example, the lowest exergy efficiency of H5 in the CFPP+CAES+CPU scheme is 42.158%, which is lower than that of the control scheme. The exergy efficiencies of H6-H8 are all higher than that of the control scheme. Among them, the highest exergy efficiency of H7 is 61.509%. Compared with the control scheme, the exergy loss of H5-H8 is reduced by 9.745kW within the daily operation cycle. As shown in Figure 4, compared with the baseline scenario, the exergy efficiencies of Heat Exchanger 1, 2, 3, and 5 at the peak period are all improved, which are 31.051%, 39.347%, 45.107%, and 47.751% respectively. The exergy efficiencies of Heat Exchanger 1 in the flat period, valley period, and peak period decrease successively, which are 48.549%, 48.415%, and 31.051% respectively. The exergy efficiency of the added heat exchanger is 79.675%. Correspondingly, the change trend of exergy loss is opposite to that of exergy efficiency, as shown in Figure 5. Within the daily operation cycle, the exergy loss of Heat Exchanger 1, 2, 3, 5, and the added components in the CFPP+CAES+CPU scheme is 2353.365kW, which reduces the exergy loss by 1499.761kW compared with the control scheme. The energy utilization capacity of the CAES waste heat utilization scheme is mainly improved by reducing the heat exchange temperature difference of the heat exchanger.

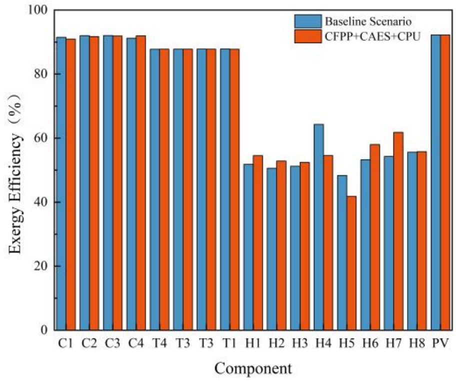

Fig.3 Exergic efficiency of CAES components

ISSN:3007-9640 DOI: https://doi.org/10.70114/acmsr.2025.3.1.P284

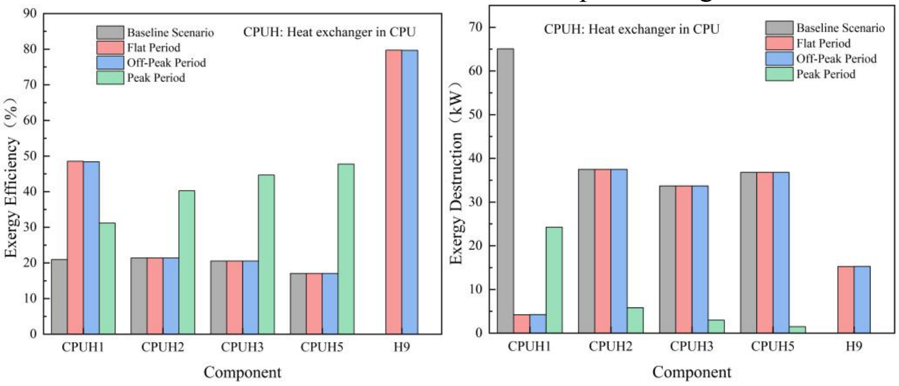

a) Exergy Efficiency b) Exergy Destruction

Fig.4 Comparison of exergic analysis of major components between the two schemes

4.4 Economic Analysis

In this paper, the economic cost of the units in the two schemes mainly consists of the oxyfuel coal-fired units and CAES, and the CAES cost is estimated by the modular cost function shown in Table 3. Due to the lack of on-site data for oxyfuel coal-fired units, scaling method [2] in economics is adopted for estimation, and the calculation formula is as follows:

$$C_i = C_{i,ref} \times \left(\frac{W_i}{W_{i,ref}}\right)^{0.74} \tag{10}$$

In the equation, C_i are the capital cost of the actual plant; $C_{i,ref}$ is the capital cost of the reference plant; W_i is the mass/energy flow rate of the actual plant; $W_{i,ref}$ is the mass/energy flow rate of the reference plant.

The construction period of this project is 2 years, and the operation period of the coupled system is 30 years. It is assumed that 45% of the fixed asset investment comes from equity, and the remaining 55% is financed by bank loans, with a long-term loan interest rate of 4.9% [17] and a short-term loan rate of 4.35%. The contingency cost is set at 5% of the fixed asset investment, and the annual inflation rate is 3%. The annual operating time during the operation period is 8,000 hours, with 12 employees and an average annual salary of ¥80,000 [16].

Coal cost is one of the main expenses of the coupled system, and this study adopts ¥500/ton [17]. In the early years of operation, there are bank interest payments. After the loan is repaid, a welfare fund is allocated at 10% of the net profit. The income tax rate is 25%, including an education surcharge of 3% and an urban maintenance and construction tax rate of 7% [16]. An annual maintenance cost of 2% of the initial investment is allocated for project maintenance. The carbon tax imposed on CO_2 emissions increases the expenses of conventional systems but has a smaller impact on coupled systems with integrated carbon capture. The carbon tax is set at ¥233.59/ton[2].

Electricity sales are the primary revenue source for the power generation system, and this study adopts the 2024 national average electricity price of ¥0.3844/kWh. The CO_2 purified by the carbon capture system can be sold as an industrial product, with a price of ¥200/ton [18]. In addition to electricity and CO_2 sales, the coupled system can trade surplus carbon emission allowances in the market, set at ¥238.42/ton in this study[2]. As an energy storage system, CAES typically participates in frequency regulation, with frequency regulation revenue accounting for 5% of the CAES investment cost [11]. In the final year of the project, the residual value of the equipment is recovered, with a net residual value rate of 5%.

Table 3 Investment costs of CAES components[7]

Component	Cost function
Compressor	$PEC = \left(\frac{39.5 m_{air}}{0.9-\eta_{AC}}\right)(\pi_{AC}) ln(\pi_{AC}) m_{air}$（kg/s）：Air mass flow rate；π_{AC}：Pressure ratio；η_{AC}Isentropic efficiency
Turbine	$PEC = \left(\frac{266.3 m_{air}}{0.92-\eta_{AT}}\right) ln(\pi_{AT})\left(1 + e^{0.36T_{in}-54.4}\right)\pi_{AT}$：Pressure ratio；$\eta_{AT}$Isentropic efficiency；$T_{in}$（k）：Inlet air temperature

ISSN:3007-9640 DOI: https://doi.org/10.70114/acmsr.2025.3.1.P284

Heat Exchanger	$PEC = 130 \times \left(\frac{A_{HEX}}{0.093}\right)^{0.78} A_{HEX}$（$m^2$）：Heat transfer area
Air Storage	$EC = 4042 \times (V_{AST})^{0.78} V_{AST}$（$m^3$）：Volume of compressed air storage
Generator	$PEC = 60 \times (1000W)^{0.95}$W（MW）：Generator output power

Since carbon emission allowances and CO_2 sales are among the revenue sources of the coupled system, while carbon tax increases its operational costs, six Mon scenarios are proposed to evaluate the impacts of these three factors on the LCOE of both schemes. The specific scenarios are detailed in Table 4.

Table 4 Consists of six Mon scenarios

Scenario	Description
Mon1	Includes carbon emission allowances, CO_2 sales, and carbon tax
Mon2	Includes carbon emission allowances and CO_2 sales
Mon3	Includes CO_2 sales and carbon tax
Mon4	Includes carbon emission allowances and carbon tax
Mon5	Includes CO_2 sales
Mon6	Includes carbon emission allowances

The LCOE of the standalone oxyfuel power plant and other schemes is calculated based on the time-of-use electricity prices in Table 1. As shown in Table 5, among the Mon1-Mon6 scenarios, the LCOE of the CFPP+CAES+CPU scheme is lower than that of the baseline scheme, indicating that the economic performance of the CFPP+CAES+CPU scheme is superior to that of the baseline scheme. The LCOE of both the baseline and CFPP+CAES+CPU schemes is lowest in the Mon2 scenario, at 0.417 ¥/kWh and 0.374 ¥/kWh, respectively. The highest LCOE for the baseline scheme occurs in Mon4, while for the CFPP+CAES+CPU scheme, it is 0.886 ¥/kWh in Mon3. This is because the latter has higher system output power than the former, resulting in greater economic benefits from carbon credit sales compared to CO_2 sales.

Table 5 LCOE comparison between the two schemes

scheme	LOCE/(¥·(kW·h)$^{-1}$)	
	the control scheme	CFPP+CAES+CPU
Mon1	0.434	0.391
Mon2	0.417	0.374
Mon3	0.865	0.860
Mon4	0.886	0.840
Mon5	0.847	0.843
Mon6	0.869	0.823

5. Summary

(1) This paper proposes a CAES-coupled oxy-fuel power plant CPU waste heat utilization scheme based on the principle of complementary energy utilization, where the waste heat from the CPU compressor replaces steam extraction for preheating turbine air. Models were developed using Ebsilon Professional and Aspen Plus software to validate the feasibility of the scheme.。

(2) By analyzing the thermodynamic performance of the scheme during peak, mid-load, and off-peak periods, it is concluded that the system output power increases in all three periods, with the highest value of 8250 kW during peak load and the lowest value of 7555.241 kW during mid-load.

(3) Through exergy analysis of system components, it is found that only the exergy efficiencies of H5-H8 in the CAES system change. Specifically, the exergy efficiency of H5 decreases, while those of H6-H8 increase. Over a daily cycle, the CFPP+CAES+CPU scheme exhibits lower exergy destruction compared to the baseline scheme；

(4) The LCOE of both the baseline and CFPP+CAES+CPU schemes is lowest in the Mon2 scenario, at 0.417 ¥/kWh and 0.374 ¥/kWh, respectively. The highest LCOE for the baseline scheme occurs in Mon4, while for the CFPP+CAES+CPU scheme, it is 0.886 ¥/kWh in Mon3. This

ISSN:3007-9640 DOI: https://doi.org/10.70114/acmsr.2025.3.1.P284
is because the latter has higher system output power than the former, resulting in greater economic benefits from carbon credit sales compared to CO2 sales.

References

[1] OLAJIRE A A. CO2 capture and separation technologies for end-of-pipe applications - A review [J]. Energy, 2010, 35(6): 2610-28 .

[2] Seo, Su Been,Kim, Hyung Woo,Kang, Seo Yeong et al.Techno-economic comparison between air-fired and oxy-fuel circulating fluidized bed power plants with ultra-supercritical cycle[J].ENERGY,2021,233,(000):121217-121217.

[3] Mao Cuiji, Yu Xiongjian, Xu Jinliang, et al. Research Progress on Key Technologies of a Flexible Peak Regulation System of Thermal Power Units Coupled with Molten Salt Thermal Energy Storage[J]. Thermal Power Generation, 2023, 52(02): 10-22.

[4] Zhang Zhu, Chen Guoqing, Zhou Xiaoming, et al. Scheme Design and Performance Analysis of a 670 MW Coal-fired Unit Coupled with a Molten Salt Energy Storage System[J]. Thermal Power Generation, 2024, 53(03): 89-98.

[5] Pang Liping, Zhang Shigang, Duan Liqiang. Research on Improving the Flexibility of a Secondary Reheat Unit by High-temperature Molten Salt Energy Storage[J]. Proceedings of the CSEE (Proceedings of the Chinese Society for Electrical Engineering), 2021, 41(08): 2682-2691.

[6] Lin Li, Yue Xiaoyu, Xu Bingqian, et al. The Calling Sequence and Strategy of the Pumped Storage-Thermal Power Joint Peak Regulation Considering the Benefits of Pumped Storage and Deep Peak Regulation of Thermal Power[J]. Power System Technology, 2021, 45(01): 20-32.

[7] Zhang, Lei,Cui, Jie,Zhang, Yanping et al.Performance analysis of a compressed air energy storage system integrated into a coal-fired power plant[J].ENERGY CONVERSION AND MANAGEMENT,2020,225,113446-113446.

[8] LI Bin, WANG Yumeng, ZHANG Qinglai, et al. Research on integrated power generation system of “solar, coal-fired power and energy storage”[J]. Thermal Power Generation, 2022, 51(2): 56-64.

[9] Jie, Pengfei,Zhao, Wanyue,Yan, Fuchun et al.Economic, energetic and environmental optimization of hybrid biomass gasification-based combined cooling, heating and power system based on an improved operating strategy[J].ENERGY,2022,240.

[10] Shi, Xingping,He, Qing,Liu, Yixue et al.Thermodynamic and techno-economic analysis of a novel compressed air energy storage system coupled with coal-fired power unit[J].ENERGY,2024,292.

[11] Li Jiajia, Li Xingshuo, Zhou Guowen, et al. Thermal Performance Analysis of Multiple Operation Modes of a Cooling, Heating and Power Tri-generation System Based on a Thermal-Storage Combined Cycle[J]. Proceedings of the CSEE, 2024, 44(09): 3598-3610.

[12] Hnydiuk-Stefan, Anna,Skladzien, Jan.Analysis of supercritical coal fired oxy combustion power plant with cryogenic oxygen unit and turbo-compressor[J].ENERGY,2017,128,271-283.

[13] LUO Wei. Research on the Optimization of Oxy-Fuel CombustionBoiler Island Control Strategy Based on Dynamic Simulation[D].Huazhong University of Science and Technology, 2016.

[14] KONG Hongbing, LIU Zhaohui, CHEN Shen et, al. Process Simulation and Optimization of a 600 MW O2 /CO2 Power Plant[J]. Proceedings of the CSEE, 2012, 32(02): 53-60.

[15] Xiong, Yong Qiang,Luo, Peng,Hua, Ben.Energy consumption analysis of air separation process for oxy-fuel combustion system[C].//4th International Conference on Chemical Engineering and Advanced Materials, CEAM 2014.2014:146-150.

[16] ZHU Yong. The Coupling Mechanism and Thermodynamic Characteristic on Solar Tower Aided Coal-fired Power Generation System[D].North China Electric Power University, 2017.

[17] CHEN Zihan. Integrated Optimization and Performance Analysis of 350MWe Oxy-combustion System[D]. Huazhong University of Science & Techology, 2021.

[18] ZHANG Zhiyu. Optimization of multi-factor parameters and coupling characteristics of oxyfuel coal-fired units with tower solar energy[D]. North China Electric Power University, 2020.